

Accepted Manuscript

Evaluation of air oxidized PAPC: A multi laboratory study by LC-MS/MS

Zhixu Ni, Bebiana C. Sousa, Simone Colombo, Catarina B. Afonso, Tania Melo, Andrew R. Pitt, Corinne M. Spickett, Pedro Domingues, M. Rosário Domingues, Maria Fedorova, Angela Criscuolo



PII: S0891-5849(19)30347-8

DOI: <https://doi.org/10.1016/j.freeradbiomed.2019.06.013>

Reference: FRB 14312

To appear in: *Free Radical Biology and Medicine*

Received Date: 28 February 2019

Revised Date: 29 May 2019

Accepted Date: 10 June 2019

Please cite this article as: Z. Ni, B.C. Sousa, S. Colombo, C.B. Afonso, T. Melo, A.R. Pitt, C.M. Spickett, P. Domingues, M. Rosá. Domingues, M. Fedorova, A. Criscuolo, Evaluation of air oxidized PAPC: A multi laboratory study by LC-MS/MS, *Free Radical Biology and Medicine* (2019), doi: <https://doi.org/10.1016/j.freeradbiomed.2019.06.013>.

This is a PDF file of an unedited manuscript that has been accepted for publication. As a service to our customers we are providing this early version of the manuscript. The manuscript will undergo copyediting, typesetting, and review of the resulting proof before it is published in its final form. Please note that during the production process errors may be discovered which could affect the content, and all legal disclaimers that apply to the journal pertain.

1 Evaluation of air oxidized PAPC: a multi laboratory study by LC-MS/MS.

2

3 Zhixu Ni^{1,2#}, Bebiana C. Sousa^{3#}, Simone Colombo⁴, Catarina B. Afonso³, Tania Melo^{4,5},
4 Andrew R. Pitt³, Corinne M. Spickett³, Pedro Domingues⁴, M. Rosário Domingues⁴, Maria
5 Fedorova^{1,2}, Angela Criscuolo^{1,2,6*}

6

7 ¹Institute of Bioanalytical Chemistry, Faculty of Chemistry and Mineralogy, University of
8 Leipzig, Germany; ²Center for Biotechnology and Biomedicine, University of Leipzig;
9 ³School of Life & Health Sciences, Aston University, Aston Triangle, Birmingham B4 7ET,
10 UK; ⁴Mass Spectrometry Centre, Department of Chemistry & QOPNA, University of Aveiro,
11 Campus Universitário de Santiago, 3810-193 Aveiro, Portugal; ⁵Department of Chemistry &
12 CESAM&ECOMARE, University of Aveiro, Campus Universitário de Santiago, 3810-193
13 Aveiro, Portugal; ⁶Thermo Fisher Scientific (Bremen) GmbH, Hanna-Kunath-Str. 11, 28199
14 Bremen, Germany.

15

16 # These authors made an equal contribution.

17

18 Corresponding author:

19 * Angela Criscuolo, Thermo Fisher Scientific (Bremen) GmbH, Hanna-Kunath-Str. 11,
20 28199 Bremen, Germany. E-mail: angela.criscuolo@thermofisher.com

21

22 Keywords

23 Oxidized phospholipids, PAPC, reverse phase chromatography, tandem mass spectrometry,
24 multi-laboratory study

25

26 Abbreviation

27 CID: collision-induced dissociation; CV: coefficient of variation; DAMP: damage associated
28 molecular pattern; DMPC: 1,2-dimyristoyl-*sn*-glycero-3-phosphocholine; HCD: high-energy
29 collisional dissociation; HOOAPC: 1-palmitoyl-2-(5-hydroxy-8-oxo-octenoyl)-*sn*-glycero-3-
30 phosphorylcholine; LC-MS/MS: Liquid chromatography coupled on-line to tandem mass
31 spectrometry; LPC: lysophosphatidylcholine; LPP: lipid peroxidation product; oxLDL:
32 oxidized LDL; oxPL: oxidized phospholipid; PAPC: 1-palmitoyl-2-arachidonoyl-*sn*-glycero-

33 3-phosphocholine; PC: phosphatidylcholine; PEIPC: 1-palmitoyl-2-epoxyisoprostaneE2-*sn*-
34 glycerol-3-phosphocholine; PGPC: 1-palmitoyl-2-glutaryl-*sn*-glycerol-3-phosphocholine;
35 POVPC: 1-palmitoyl-2-(5-oxovaleroyl)-*sn*-glycerol-3-phosphorylcholine; PL: phospholipid;
36 TS: truncation score; XIC: Extracted ion chromatograms.

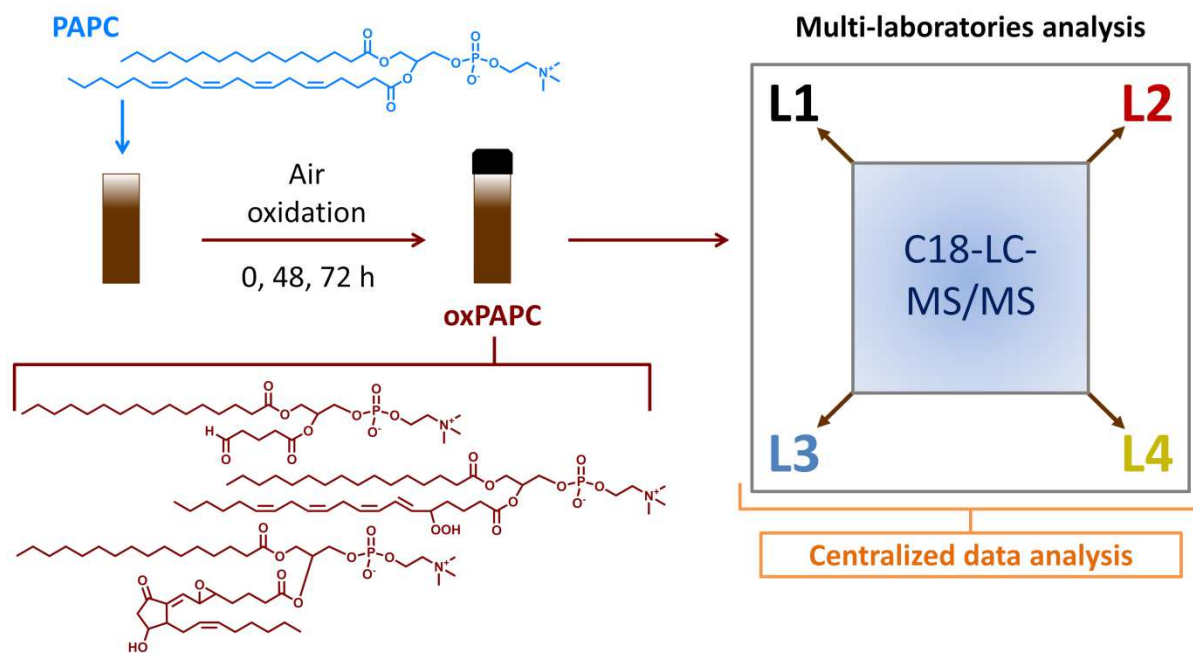
37

38 **Abstract**

39 Oxidized LDL (oxLDL) has been shown to play a crucial role in the onset and
40 development of cardiovascular disorders. The study of oxLDL, as an initiator of
41 inflammatory cascades, led to the discovery of a variety of oxidized phospholipids (oxPLs)
42 responsible for pro-inflammatory actions. Oxidized 1-palmitoyl-2-arachidonoyl-*sn*-glycerol-3-
43 phosphocholine (PAPC) is frequently used by the scientific community as a representative
44 oxPL mixture to study the biological effects of oxidized lipids, due to the high abundance of
45 PAPC in human tissues and the biological activities of oxidized arachidonic acids derivatives.
46 Most studies focusing on oxPAPC effects rely on in-house prepared mixtures of oxidized
47 species obtained by exposing PAPC to air oxidation. Here, we described a multi-laboratory
48 evaluation of the compounds in oxPAPC by LC-MS/MS, focusing on the identification and
49 relative quantification of the lipid peroxidation products (LPPs) formed. PAPC was air-
50 oxidized in four laboratories using the same protocol for 0, 48, and 72 hours. It was possible
51 to identify 55 different LPPs with unique elemental composition and characterize different
52 structural isomeric species within these. The study showed good intra-sample reproducibility
53 and similar qualitative patterns of oxidation, as the most abundant LPPs were essentially the
54 same between the four laboratories. However, there were substantial differences in the extent
55 of oxidation, i.e. the amount of LPPs relative to unmodified PAPC, at specific time points.
56 This shows the importance of characterizing air-oxidized PAPC preparations before using
57 them for testing biological effects of oxidized lipids, and may explain some variability of
58 effects reported in the literature.

59 **Graphical Abstract**

60

61
62

ACCEPTED MANUSCRIPT

63 1. Introduction

64 The role of oxidized LDL as an initiator of inflammatory cascades that contribute to the
65 pathogenesis of cardiovascular disorders including atherosclerosis, led to the discovery of a
66 variety of oxidized phospholipids (oxPLs) important for the fine tuning of innate and
67 adaptive immune responses [1–3]. OxPLs formed via enzymatic or free-radical driven
68 reactions are closely associated with systemic redox imbalance and low-grade chronic
69 inflammation, and thus have been intensively studied from structural, chemical, biophysical,
70 and biological perspectives over the last decades[4–8]. Within the generic classification of
71 oxPL, the oxidation products of 1-palmitoyl-2-arachidonoyl-*sn*-glycero-3-phosphocholine
72 (PAPC), which have been identified as some of the bioactive components in minimally
73 modified LDL, are the oxPLs most often used to study the biological effects of oxidized
74 lipids [9]. Furthermore, PAPC is among the most abundant PLs in human tissues [10].
75 Arachidonic acid, present in the *sn*-2 position of PAPC, can form a very diverse range of
76 oxidation products, many of which have already been shown to be bioactive in their free fatty
77 acid forms. Indeed, numerous studies have demonstrated the pro- and anti-inflammatory
78 properties of, for example, eicosanoids, which are generated from arachidonic acid via action
79 of dedicated enzymes or free radical driven lipid peroxidation [11–13]. However, the action
80 of PC-esterified eicosanoids has been relatively less well studied.

81 A variety of bioactivities have been attributed to oxidized PAPC (oxPAPC). It has been
82 identified as a major pro-atherogenic factor and pro-inflammatory mediator [14,15], but in
83 contrast anti-inflammatory properties of oxPAPC have also been demonstrated [13,16].
84 OxPAPC has been shown to induce both the disruption as well as enhancement of the
85 endothelial barrier [17,18], and recently a pro-algesic effect of oxPAPC, via stimulation of
86 transient receptor potential channels TRPA1 and TRPV1, was demonstrated [19,20].
87 OxPAPC was also shown to act as a damage associated molecular pattern (DAMP),
88 activating classical and non-classical pattern recognition receptors. Thus, oxPAPC released
89 from injured tissues was shown to be recognized by murine caspase-11 and CD14 leading to
90 inflammasome activation and release of pro-inflammatory cytokines, and this pathway
91 demonstrated differential regulation in macrophages and dendritic cells [21–23]. The variety
92 of biological effects of oxPAPC are well established and their conflicting properties have
93 been discussed recently [24–26].

94 One of the main obstacles in elucidating the effects oxPLs on biological systems is the
95 almost complete lack of commercially available and chemically characterized standards for
96 each individual oxPL product. Thus, to study their biological properties, a mixture of

97 products, usually referred to as “oxPAPC” is often used. The majority of the studies on
98 oxPAPC effects rely on commercial or in-house preparations, usually obtained by exposing a
99 dried film of PAPC to air oxidation for up to 72 h. Experimental details such as room
100 temperature, light exposure, thickness of the phospholipid film and oxPAPC quality control
101 are usually not provided. Given the variety of biological functions attributed to oxPAPC in
102 different cellular and *in vivo* models, which may be dependent on variations in sample
103 preparation affecting the precise composition of the oxPAPC, we performed a multi-
104 laboratory study with the aim of evaluating the reproducibility of PAPC oxidation upon air
105 exposure for 48 and 72 h. Liquid chromatography coupled on-line to tandem mass
106 spectrometry (LC-MS/MS) was used to identify lipid peroxidation products (LPPs) formed
107 upon PAPC oxidation, and the relative quantities of LPPs formed were compared between
108 samples generated independently in four different international laboratories.

109 110 **2. Materials and Methods**

111 **2.1. Materials**

112 1-palmitoyl-2-arachidonoyl-sn-glycero-3-phosphocholine and 1,2-dimyristoyl-sn-
113 glycero-3-phosphocholine were purchased from Avanti Polar Lipids (Avanti Polar Lipids,
114 Inc., Alabama, USA). In laboratory 1 (L1) acetonitrile, isopropanol, water, methanol,
115 ammonium formate (Optima LC-MS grade), chloroform and formic acid (LC-MS grade)
116 were obtained from Fisher Scientific (Loughborough, UK). In laboratory 2 (L2) HPLC-MS
117 grade chloroform, methanol, acetonitrile and isopropanol were purchased from Fisher
118 Scientific (Leicestershire, UK). Formic acid was from Honeywell Fluka (Neu Wulmstorf,
119 Germany). Ammonium formate was obtained from Sigma-Aldrich (Sigma-Aldrich, Munich,
120 Germany). The water was of Milli-Q purity (Synergy1, Millipore Corporation, Billerica,
121 MA). In laboratory 3 (L3) acetonitrile, isopropanol, water, methanol, ammonium formate
122 (Optima™ LC/MS grade) and chloroform (LC/MS grade) were obtained from Fisher
123 Scientific (Schwerte, Germany). Formic acid (LC-MS grade) was purchased from Sigma-
124 Aldrich (Sigma-Aldrich, Munich, Germany). In laboratory 4 (L4) acetonitrile, isopropanol,
125 methanol, and formic acid (all ULC-MS grade) were from Biosolve (Valkenswaard,
126 Netherlands). Ammonium formate and chloroform were from Sigma-Aldrich GmbH
127 (Taufkirchen, Germany).

128 **2.2. OxPAPC preparation.**

129 OxPAPC was prepared either in one laboratory (L3) or independently in four
130 participating laboratories following the protocol describe below. A mixture of 1-palmitoyl-2-

131 linoleoyl-*sn*-glycero-3-phosphocholine (PAPC; 50 µg) and 1-2-dimiristoyl-*sn*-glycero-3-
132 phosphocholine (DMPC; 2.2 µg; a fully saturated PC used as internal standard for relative
133 quantification) in chloroform was dried under a stream of N₂ in a 2 mL amber flat bottom vial
134 to form a thin film at the vial bottom (three independent replicates). The lipid film was
135 exposed to air at room temperature (L1 – 22-25°C, L2 – 16°C, L3 – 28°C, L4 – 25°C) for 0,
136 48 and 72 hours. After incubation the vial was filled with N₂, tightly sealed and stored at -
137 80°C. Samples from L3 were sent to the other laboratories on freezer blocks at -20°C .

138 **2.3. LC-MS/MS analysis.**

139 The experimental replicates (n=3) of sample prepared in L3 (0 and 72 h of oxidation;
140 analysed by L1, L3, and L4), as well as samples generated independently in each of the four
141 participating laboratories and analysed there, were used to assess inter-laboratory variability.
142 In L4, experimental replicate 1 was analysed in triplicate on three consecutive days, to assess
143 intra- and inter-day analytical variability. Comparable chromatographic conditions and the
144 best available tandem MS instrument were used in the 4 laboratories. Details on LC-MS/MS
145 are provided in **Table 1** and Supplementary Methods section. Briefly, UHPLC separations
146 were performed on C18 reverse phase columns using binary solvent systems containing
147 water, acetonitrile, methanol and isopropanol, with ammonium formate (5 mmol/L) and
148 formic acid (0.1%) as additives [27]. MS analyses were performed using data-dependent
149 acquisition (DDA) in positive and negative ion modes (**Table 1** and Supplementary
150 Methods).

151 **2.4. Automated identification of lipid peroxidation products (LPPs).**

152 LPPtiger software source code version was used for lipid identification ([28];
153 <https://bitbucket.org/SysMedOs/lpptiger>). PAPC was oxidized *in silico* using theoretical
154 oxidation level 2. The list of modifications included hydroperoxy, hydroxy, epoxy, and keto
155 groups with the maximum number equal to the number of bis-allylic and allylic sites in the
156 structure. The oxidative cleavage products with aldehyde and carboxylic acid on the terminal
157 carbon were included. LPPtiger predicted 345 unique oxidized fatty acyl chains
158 corresponding to 692 discrete oxPAPC species including lyso species. All raw spectra were
159 converted into mzML format using ProteoWizard MSconvert (Version 3.0.9134 64bit) and
160 the following parameters were used for all files: *m/z* range 400 to 1000, isotope score filter
161 80, and overall score filter 40. For L1 files 50 ppm on MS level and 200 ppm on MS2 level
162 were used as mass tolerance thresholds. For L2, L3, and L4 mass tolerance of 10 ppm on MS
163 and MS2 levels was applied. Analysis was performed using the integrated batch mode of
164 LPPtiger on a workstation equipped with 2 CPUs (32 cores) and 128 GB of RAM in L4.

165 2.5. Relative LPPs quantification.

166 15 LPPs detected in all four laboratories and previously reported in the literature as a
167 component of oxPAPC [9,11,13,14,16–18,23,29,30] were chosen for the relative
168 quantification (Table 2). Peak area for each lipid was integrated and normalized relative to
169 the DMPC lipid used as non-oxidizable internal standard. Average percent values for each
170 LPP relative to PAPC were calculated using normalized peak areas.

171 2.6. Statistical analysis.

172 Coefficient of variation (CV%) was calculated using the following equation $CV\% =$
173 $DevSTD/AverageRelativeArea*100$ for each LPPs using normalized peak areas. Principal
174 component analysis was performed using normalized peak area of 15 LPPs from L3 prepared
175 samples analyzed by three laboratories (L1, L3 and L4) using EZinfo (version 1.0, MKS
176 Instruments, Crewe, UK). ANOVA (Single Factor) analysis was performed by Analysis
177 ToolPak Excel Add-In for each LPPs using normalized peak areas.

178 2.7. Nomenclature.

179 Lipid nomenclature is based on the LIPID MAPS consortium recommendations [31].
180 For instance, the shorthand notation PC 36:4 represents a phosphatidylcholine lipid
181 containing 36 carbons and four double bonds. When the fatty acid identities and *sn*-position
182 are known, as in our case, the slash separator is used (e.g., PC 16:0/20:4). Since no unified
183 nomenclature is available for oxidized lipids, the short hand notations provided by LPPtiger
184 tool were used [28]. Short chain oxidized lipids were indicated by the corresponding terminal
185 enclosed in angular brackets (e.g. “<” and “>”), with the truncation site indicated by the
186 carbon atom number (e.g., <COOH@C9> and <CHO@C12>). For long chain products our
187 recommendation is to indicate the number of oxygen addition after the fully identified parent
188 lipid (e.g. PC 16:0/20:4 + 1O) when the type of addition is not known, or in parenthesis for
189 known functional groups (e.g. PC 16:0/20:4[1xOH@C11]).

190
191
192
193
194
195
196

197 **Table 1.** Summary of LC-MS/MS methods used for the analysis of oxPAPC in four different
 198 laboratories.

	L1	L2	L3	L4
Chromatography				
Column	Accucore™ C18	ACE C18	Accucore™ C18	Accucore™ C18
Column phase	Solid core, C18	Solid core, C18	Solid core, C18	Solid core, C18
Dimensions	150 x 2.1 mm	150 x 0.5 mm	150 x 2.1 mm	150 x 2.1 mm
Particle size	2.6 μm	5 μm	2.6 μm	2.6 μm
Pore size	150 Å	100 Å	150 Å	150 Å
Gradient	isopropanol: acetonitrile: water	isopropanol: methanol: acetonitrile: water	isopropanol: acetonitrile: water	isopropanol: acetonitrile: water
Temperature	50 °C	40 °C	50 °C	50 °C
Tandem MS				
Instrument	5600 TripleTOF	Q Exactive™	Orbitrap Fusion™ Lumos™ Tribid™	Q Exactive™ Plus
MS1	200-1500 <i>m/z</i>	400–1200 <i>m/z</i>	450–1200 <i>m/z</i>	380–1200 <i>m/z</i>
Resolution	High sensitivity	70,000	120,000	140,000
DDA top #	5	5	15	10
Fragmentation	CID	HCD	HCD	HCD
CE	35V, 10V CES	NCE 20, 23, 25	NCE 20 +/- 10	NCE 18 +/- 6
Resolution MS2	High sensitivity	17,500	15,000	17,500

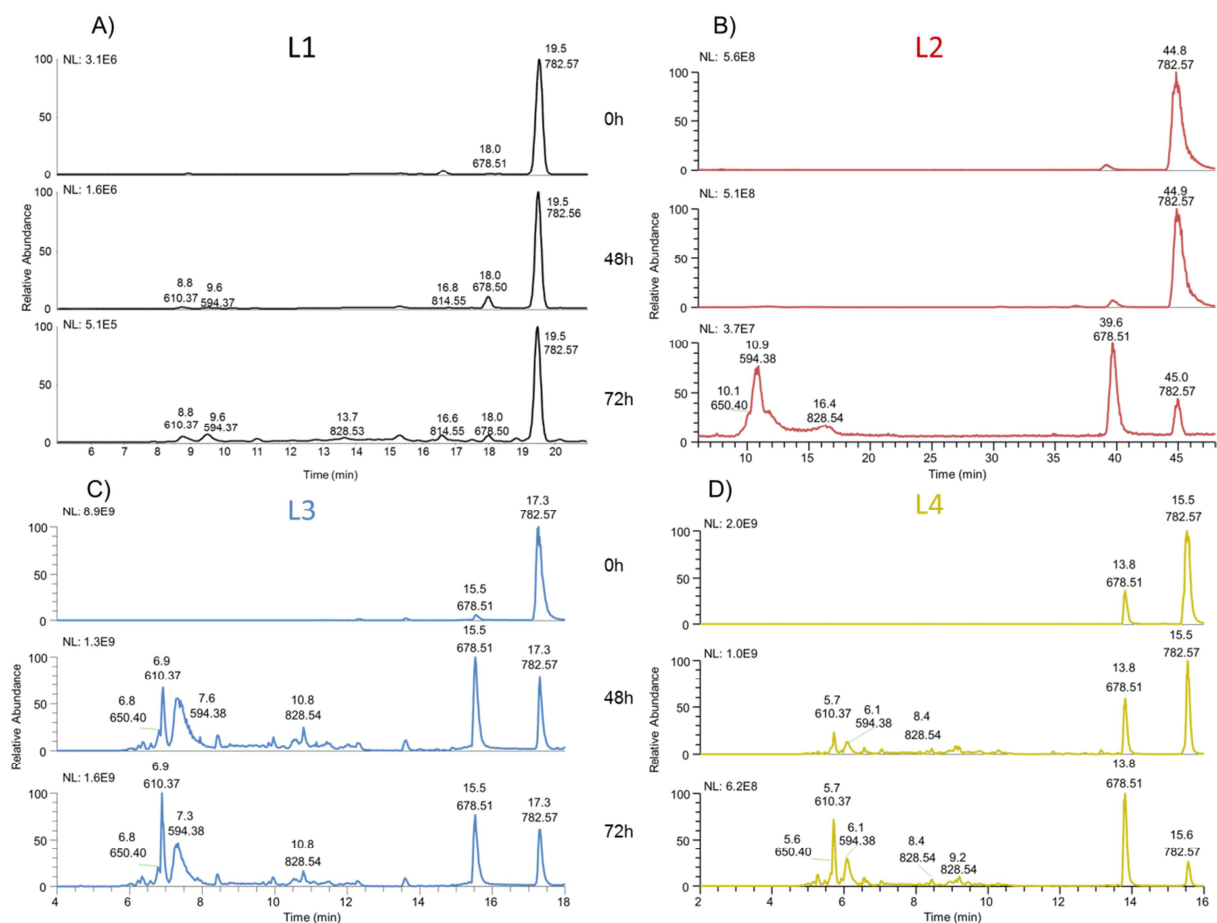
199

200 3. Results and Discussion

201 3.1. Identification of LPP species in air oxidized PAPC.

202 To evaluate the extent of PAPC oxidation and identify the LPPs formed, oxPAPC
203 samples prepared in four different laboratories (L1-L4) were analysed by LC-MS/MS using
204 reverse phase separation on C18 columns and data-dependent acquisition on four different
205 MS instruments (**Table 1**). OxPAPC mixtures were analysed in both positive and negative
206 ion modes. Positive ion mode data were used for relative quantification, given the higher
207 ionization efficiency of PC lipids as protonated quasi-molecular ions, whereas the negative
208 ion mode data were used for identification of LPPs based on tandem mass spectra of the
209 formate adduct or deprotonated ions, as the negative ion fragmentation data contains
210 informative fragment anions of the modified acyl chains.

211 **Fig. 1** shows representative positive ion mode base peak chromatograms for three
212 different time points of PAPC oxidation obtained from the four laboratories. Representative
213 negative ion mode base peak chromatograms are shown in **Supplementary Fig. S1**. DMPC,
214 which contains two fully saturated C14:0 acyl chains, was spiked into all preparation at equal
215 quantities (PAPC:DMPC, 20:1 molar ratio) and was used as an internal standard for relative
216 quantification. The general pattern of oxidation was very similar between all laboratories. At
217 the 0 h time point two main signals, corresponding to DMPC (m/z 678. 51⁺) and native PAPC
218 (m/z 782. 57⁺), are clearly visible, with almost a complete absence of LPPs. After 48 h of air
219 exposure, a large number of signals for analytes with shorter retention times than PAPC can
220 be observed, indicating the presence of species with higher polarities than native PAPC. After
221 72 h, most of the signals eluted towards the beginning of chromatographic gradients,
222 generally in the first third, corresponding to chain-shortened oxidation products, accompanied
223 by a corresponding decrease of the signals eluting in the middle third of the gradient,
224 corresponding to long-chain oxidised products, as well a decrease the native PAPC signal
225 which appears towards the end of the gradient.



226

227 **Fig. 1.** Positive ion mode base peak chromatograms of PAPC lipid oxidized by air exposure
 228 for 0, 48 and 72 h and analysed using reverse phase chromatography coupled on-line to
 229 tandem mass spectrometry detection in L1 (A), L2 (B), L3 (C) and L4 (D).

230

231 LPPtiger, a new software for the identification of oxidized phospholipids from data-
 232 dependent LC-MS/MS datasets, was used for the automated identification of LPPs in the
 233 oxPAPC preparations [28]. LPPtiger performs identification based on the fragment ions
 234 observed in CID or HCD experiments in the negative ion mode. The presence of specific
 235 anions corresponding to native and oxidized acyl chains in PLs allows identification of the
 236 oxidation type, whereas fragment ions and specific neutral losses provides identification of
 237 PL class. Identification of positional isomers of oxPL is not supported by the current version
 238 of the software, but the MS/MS based identification of oxidized fatty acyl chains together
 239 with isotopic scores correction provide a solid basis for the identification of molecular
 240 species.

241 Overall 55 different LPPs with unique elemental compositions were identified,
 242 providing 143 potential LPPs after considering functional group isomers (**Supplementary**

243 **Table S1**). The 55 identified LPPs covered a number of different types of oxidative products,
244 including the lysophosphatidylcholines (LPC) LPC(16:0) and LPC(20:4), as well as 40 short
245 chain and 15 long chain LPPs. 24 LPPs were identified by all three laboratories that
246 performed DDA analysis (L2 used an inclusion list function and thus was not considered for
247 this comparison), and 45 LPPs were identified by two laboratories. Overall, all of the main
248 LPPs generally regarded as being present in oxPAPC mixtures were successfully identified
249 by LPPtiger at the MS/MS level, including the truncated species 1-palmitoyl-2-(5-
250 oxovaleroyl)-*sn*-glycero-3-phosphorylcholine (POVPC; m/z 594.38⁺) and 1-palmitoyl-2-
251 glutaryl-*sn*-glycero-3-phosphocholine (PGPC; m/z 610.37⁺), long chain products with
252 hydroperoxy, hydroxy, and keto groups, and 1-palmitoyl-2-epoxyisoprostanE2-*sn*-glycero-
253 3-phosphocholine (PEIPC; m/z 828.54⁺).

254 The different numbers of LPPs identified by LPPtiger from the MS/MS data from the
255 four laboratories most probably relates to the differences in MS methods and instruments
256 used in the study. Thus, the highest number of LPPs was identified by L3 utilizing a Tribid
257 Orbitrap Fusion Lumos, which is capable of acquiring a high number of tandem mass spectra
258 (15 MS/MS) per one survey scan, followed by L4 and L1 in which top 10 and top 5 DDA
259 methods were applied using a Q Exactive™ Plus and a TripleToF 5600 respectively. L2
260 performed targeted acquisition using inclusion lists for 63 LPPs, of which 12 were
261 successfully identified.

262 3.2. LC-MS/MS based identification of isomeric LPPs.

263 Reverse phase chromatographic separation allowed the resolution of multiple isomeric
264 LPP species. The C18 phase proved to be a good stationary phase for the separation of the
265 relatively polar analytes formed by the oxidation of PLs, which are characterized by a mid-
266 range polarity compared to the other lipid classes. Reverse phase separation strongly depends
267 on the hydrophobicity of the analyte, usually described by the partition coefficients logP and
268 logD [32], along with to a lesser extent some other physico-chemical properties, such as
269 dipole-dipole interactions, proton acceptor/donor interactions and analyte polarizability. In
270 comparison with native PAPC, which has a logP 8.4, introduction of a single hydroxy group
271 results a shift of the logP to 7.2, whereas presence of three hydroxy groups or the isoprostanE
272 ring structures (e.g. PGF2 α) further shifts the logP values further to 5.1 and 4.5, respectively.
273 The use of a C18 stationary phase with an isopropanol-acetonitrile-water elution gradient
274 ensures optimal binding of these mid-polarity lipid analytes while still providing efficient
275 separation of lipid species. The combination of LC separation with tandem mass

276 spectrometry allows the acquisition of separate tandem mass spectra for the separated
277 isomeric LPPs, and CID or HCD fragment spectra acquired in the negative ion mode
278 provides the information necessary to identify the type and often the position of the
279 modification.

280 **Fig. 2** illustrates three examples of LC-MS/MS based identification of short chain
281 oxPAPC species.

282 Extracted ion chromatograms (XICs) for POVPC (**Fig. 2**) in negative ($[M+HCOOH-$
283 $H^+]$, m/z 638.37) and positive ($[M+H^+]$, m/z 594.38) ion modes both had two
284 chromatographic peaks with a retention times of 5.6 and 6.1 min. Although the POVPC
285 signal was already present at the 0 h oxidation time point, the intensity of this LPP increased
286 by more than two orders of magnitude over the oxidation time course (e.g. from $5e4$ counts at
287 0h to $8e6$ counts at 72 h for the example shown in **Fig. 2** of the analysis performed by L3).
288 The positive mode HCD tandem mass spectra showed the presence of the fragment ion
289 characteristic of the PC head group at m/z 184, whereas the negative ion mode tandem mass
290 spectra acquired at 5.1 and 6.1 min provided more detailed information on LPP structure. For
291 example, the fragment ion at m/z 578.35 corresponded to the loss of formate and a methyl
292 group, a characteristic loss for the PC head group. The most informative region was where
293 anions of palmitic acid (m/z 255.23) and the five carbon long modified acyl chain with a C5
294 terminal aldehyde could be detected (m/z 155.04). The differences in MS/MS spectra taken at
295 the different retention times can most likely be attributed to the *sn-1/sn-2* positions of the two
296 fatty acyl chains. Thus, the most intense signal eluting at 6.1 min most probably corresponds
297 to 1-palmitoyl-2-(5-oxovaleroyl)-*sn*-glycero-3-phosphorylcholine whereas the signal at 5.6
298 min, which has a higher intensity of the m/z 115.04 ion, is probably due to the positional
299 isomer 1-(5-oxovaleroyl)-2-palmitoyl-*sn*-glycero-3-phosphorylcholine [33,34]. Similarly,
300 two chromatographic peaks were observed in the XIC at the mass of PGPC (**Supplementary**
301 **Fig. S2**), and the XICs generated from both positive and negative mode data showed up to a
302 three orders of magnitude increase in PGPC signal over the oxidation time course. The
303 fragmentation data showed a different ratio between the anionic acyl chain fragment
304 intensities (m/z 255.23 for palmitic and m/z 113.02 and 145.05 for glutaric acid), and the
305 fragmentation spectra in negative ion mode were characterized by the diagnostic neutral loss
306 of 59 Da from the parent (fragment at m/z 549.28), corresponding to loss of CH_3COOH from
307 a terminal carboxylic acid, and the two fragment ions related to the short chain oxidized FA
308 (m/z 113.02 and 145.05). These fragmentations with a Δm of 32 Da are due to the
309 rearrangement of the polar head group, as has been described previously [35].

310

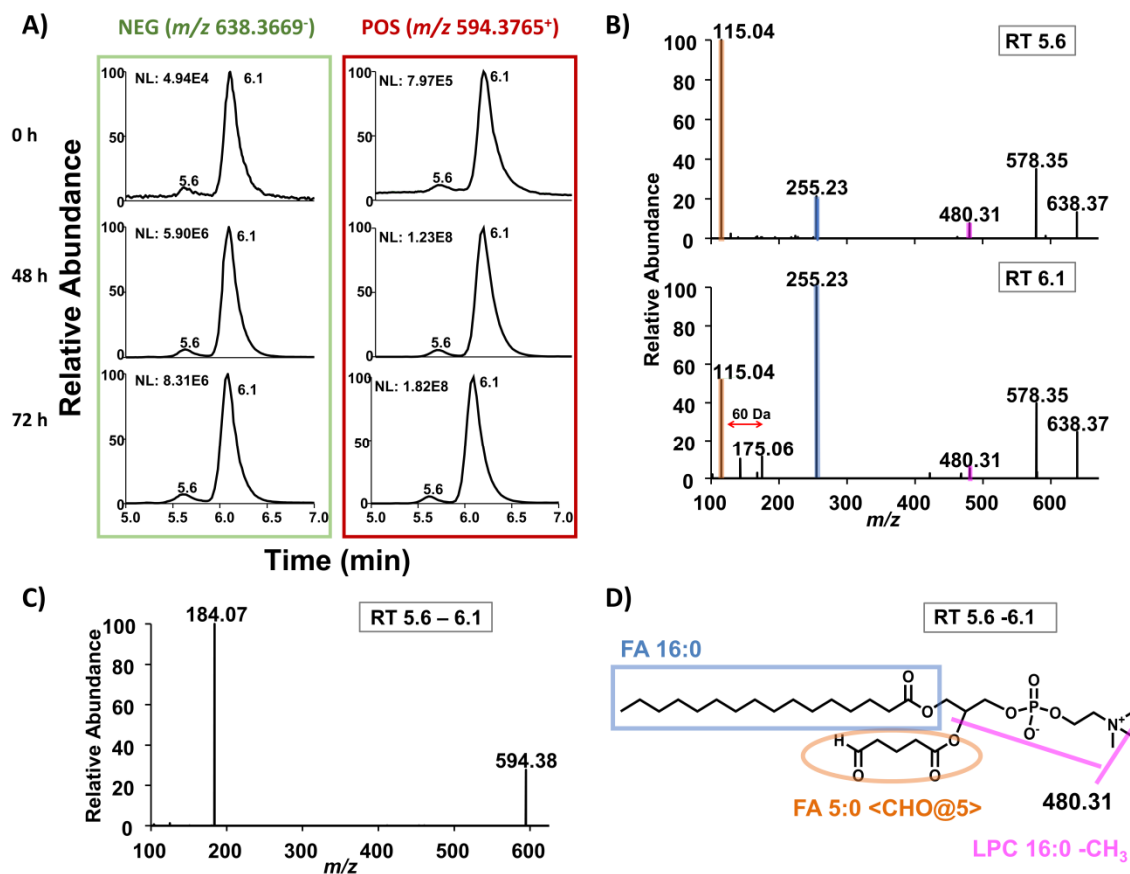
311 1-palmitoyl-2-(5-hydroxy-8-oxo-octenoyl)-*sn*-glycero-3-phosphorylcholine
312 (HOOAPC), a previously reported short chain oxidized lipid in oxPAPC preparations, was
313 also already present at time 0 h, and increased with time by up to two orders of magnitude
314 (**Supplementary Fig. S3**). Once more, it was possible to identify the presence of two
315 chromatographic peaks showing a different ratio between the intensities of the acyl chain
316 anion signals. The loss of formate and methyl groups in negative ion mode and the polar head
317 group PC characteristic fragments in positive ion mode were observed. A diagnostic ion
318 confirming the hydroxyl group to be on an eight carbon long truncated acyl chain was present
319 at m/z 153.06, resulting from water loss relative to the short chain oxidized FA (m/z 171.07).

320 **Fig. 3** shows three examples of LC-MS/MS based identification of long chain oxPAPC
321 species. In this case, the XICs are much more complex than for the short chain LPPs,
322 indicating the presence of multiple isomeric species. For example, at least 11 different
323 chromatographic peaks, 8 of them showing baseline separation, were detected for a mass
324 corresponding to PAPC with the addition of one oxygen (**Fig. 3**). Furthermore, the
325 chromatographic profile differed at the three oxidation time points. At 0 h all 11 peaks were
326 present, while after 72 h some had disappeared. The fragmentation spectra in positive ion
327 mode showed, as expected, a major fragment ion from the PC head group, but it was also
328 possible to see a fragment ion resulting from the loss of 18 Da, corresponding to the loss of
329 H₂O which is diagnostic of an OH group. Negative ion mode tandem mass spectra allowed
330 the identification of many of the modification isomers. Thus, the isomeric PAPC oxidation
331 products with a hydroxy (RT 13.1) or an epoxy (RT 13.9) group were identified based on the
332 diagnostic ions at m/z 127.08 and 155.07 respectively, with the hydroxy group identified as
333 being at position C7, and the epoxy group at C5-C6 (from the ion at m/z 191.18).

334 **Supplementary Fig. S4** shows the identification of PAPC with the addition of two
335 oxygens, where the XIC shows six main peaks at time points 0 h and 48 h, while at 72 h
336 additional chromatographic peaks with shorter retention times were present. In positive ion
337 mode the earlier eluting peaks showed one and two neutral losses of water molecules (-18
338 and -36 Da), typical of diHETE derivatives, while the later eluting signals were characterized
339 by the neutral losses of 18 and 34 Da, diagnostic of lipid hydroperoxides. Furthermore, with
340 these species for the first time we could identify in negative ion mode a diagnostic fragment
341 ion (m/z 335.22) from the diHETE-PC, corresponding to arachidonic acid carrying two
342 hydroxyl groups, whereas for the hydroperoxide containing oxPAPC the predominant signal
343 was detected at m/z 317.21 (single water loss). Occasionally, it was even possible to detect a

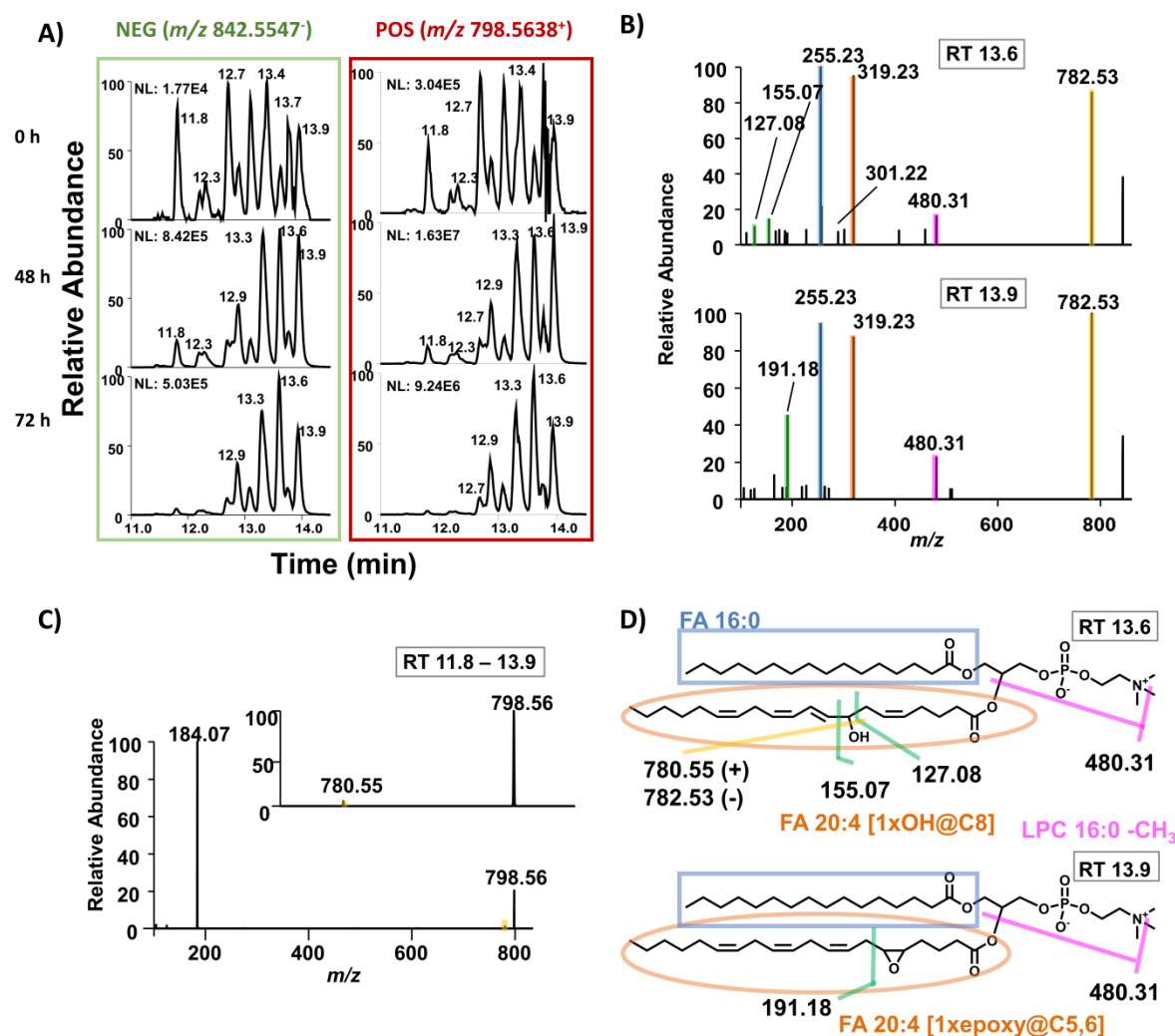
344 signal at m/z 331.23 corresponding to [FA 20:4 + OOH - 2H] and characteristic fragments
345 ions at 203.18 and 129.06 m/z , diagnostic for a hydroperoxide group at position C5.

346 **Supplementary Fig. S5** demonstrates the identification of a long chain oxidized PAPC
347 derivative characterized by the addition of three oxygen atoms and the loss of two hydrogens.
348 The intensity over the oxidation time course increased by one order of magnitude between 0
349 and 48 h and then remained approximately constant. The most studied product with this mass
350 is PEIPC. The fragmentation spectrum in negative ion mode is shown in **Supplementary**
351 **Fig. 5B**. All previously reported [36] diagnostic fragment ions were present (m/z 331.19,
352 313.18, 305.21, 287.21, 269.19), including the characteristic ions for the epoxy group at the
353 position C5-C6 (m/z 233.15, 215.14, 203.14, 147.07, 115.04). In positive ion mode the
354 fragmentation spectra were characterized by the PC-specific fragment ion (184.07 m/z) and
355 diagnostic OH neutral losses (loss of 18 and 36 Da).



356

357 **Fig. 2.** Extracted ion chromatograms (A), HCD tandem mass spectra in negative (B), and
 358 positive ion modes (C) and proposed structure (D) of POVPC. Color-coding of structure-
 359 related signals in the negative mode MS/MS spectra (e.g. the anion of FA 16:0 in blue, oxFA
 360 in orange and green, and LPC fragment derived as NL of one FA in pink) corresponds to the
 361 color-coding of fragments assigned to proposed structures illustrated in the lower panel.



362

363 **Fig. 3.** Extracted ion chromatograms (A), HCD tandem mass spectra in negative (B), and
 364 positive ion mode (C) and proposed structure (D) of PAPC with the addition of one oxygen.
 365 Color-coding of structure-related signals in negative mode MS/MS spectra (e.g. the anion of
 366 FA 16:0 in blue, oxFA in orange and green, and LPC fragment derived as NL of one FA in
 367 pink) corresponds to the color-coding of fragments assigned to proposed structures illustrated
 368 in the lower panel.

369 3.3. Relative quantification of LPPs in air oxidized PAPC

370 15 LPPs, including lyso PCs (LPCs), short and long chain oxidation products, were
 371 selected for relative quantification (**Table 2**). Before evaluating the reproducibility of PAPC
 372 air oxidation in the four different laboratories, intra- and inter-laboratory analytical variability
 373 was examined.

374

375 **Table 2.** Elemental composition and proposed structures for the 15 LPPs in the oxPAPC
 376 mixture used for quantification. For each LPP the exact mass and m/z values for
 377 corresponding formate adduct (or m/z deprotonated ions in case of short chain LPPs with
 378 carboxylic acid terminal groups, marked with *) and protonated ions are provided.

Formula_ Neutral	Proposed structures	Exact mass	neg m/z [M +HCOO] ⁻	pos m/z [M+H] ⁺
C ₂₄ H ₅₀ NO ₇ P	LPC(16:0)	495.3325	540.3307	496.3398
C ₂₈ H ₅₀ NO ₇ P	LPC(20:4)	543.3325	588.3307	544.3398
C ₂₉ H ₅₆ NO ₉ P	PC(16:0/5:0<CHO@C5>)	593.3692	638.3669	594.3670
C ₂₉ H ₅₆ NO ₁₀ P	PC(16:0/5:0<COOH@C5>)	609.3636	608.3564*	610.3715
C ₃₂ H ₆₀ NO ₁₀ P	PC(16:0/8:1[1OH]<CHO@C8>)	649.3949	694.3931	650.4022
C ₃₄ H ₆₂ NO ₉ P	PC(16:0/10:2<CHO@C10>)	659.4157	704.4139	660.4235
C ₃₇ H ₆₆ NO ₉ P	PC(16:0/13:3<CHO@C13>)	699.4470	744.4452	700.4548
C ₄₄ H ₇₈ NO ₉ P	PC(16:0/20:4) +1O – 2H	795.5409	840.5391	796.5482
C ₄₄ H ₈₀ NO ₉ P	PC(16:0/20:4) +1O	797.5565	842.5547	798.5638
C ₄₄ H ₇₆ NO ₁₀ P	PC(16:0/20:4) +2O – 4H	809.5201	854.5183	810.5274
C ₄₄ H ₈₀ NO ₁₀ P	PC(16:0/20:4) +2O	813.5514	858.5496	814.5587
C ₄₄ H ₇₈ NO ₁₁ P	PC(16:0/20:4) +3O – 2H	827.5307	872.5289	828.5380
C ₄₄ H ₈₀ NO ₁₁ P	PC(16:0/20:4) +2O	829.5464	874.5446	830.5536
C ₄₄ H ₈₀ NO ₁₂ P	PC(16:0/20:4) +4O	845.5413	890.5395	846.5486
C ₄₄ H ₇₈ NO ₁₃ P	PC(16:0/20:4) +5O – 2H	859.5205	904.5187	860.5284

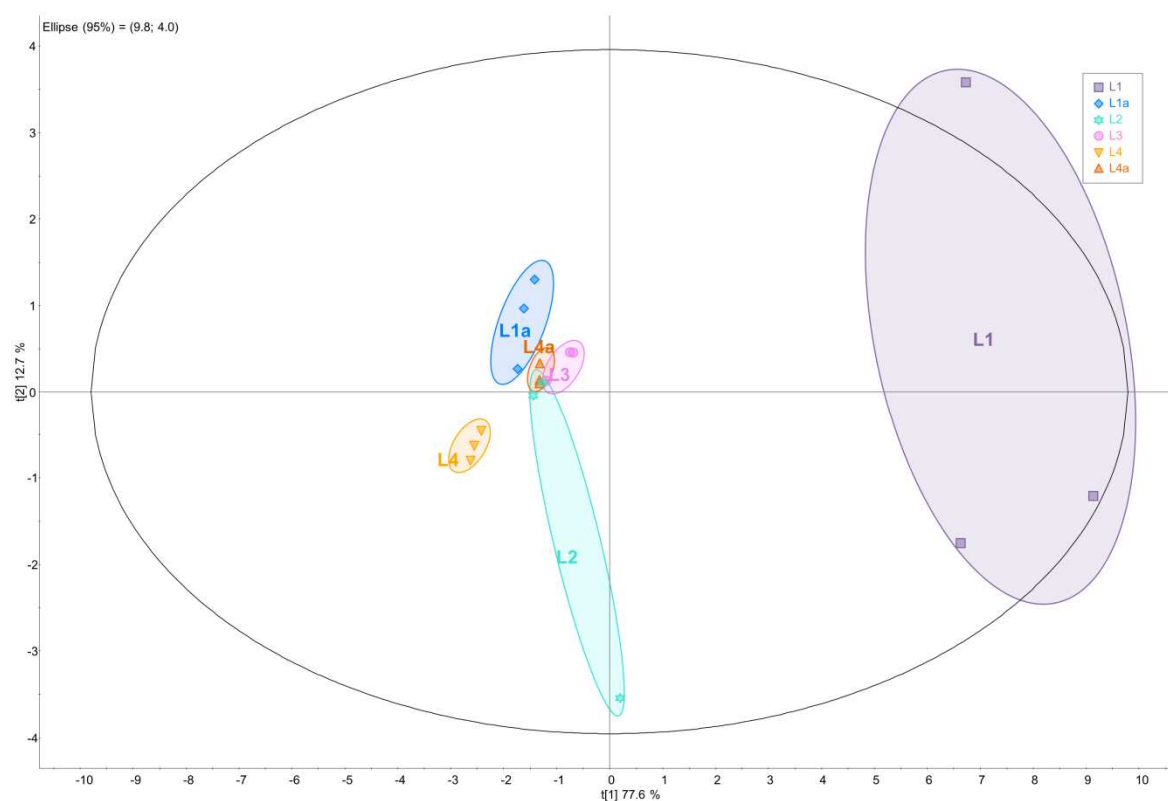
379

380 The LC-MS method used for relative LPP quantification had already been validated in
381 different laboratories for the analysis of complex lipidomes [27,37]. To provide an estimation
382 of the likely intra-lab accuracy of the quantification results for the LPPs, L4 evaluated intra-
383 sample as well as analytical variation (CV%) by analyzing one experimental replicate of the
384 oxPAPC preparation for each oxidation time point on three consecutive days. Normalized
385 peak areas were calculated for both positive and negative ion modes (**Supplementary Table**
386 **S2**). The coefficient of variation was under 20% for all LPPs at all time points, except for
387 LPCs at time 0 h, which showed higher inter-day variability (up to 34%), probably as the
388 storage of the oxPAPC sample over 3 days at -80 °C does not prevent the oxidation or
389 hydrolysis process completely.

390 To assess inter-laboratory analytical variance, oxPAPC samples generated in L3 (0 and
391 72h oxidation) were analyzed in three different laboratories (L1, L3 and L4). Normalized
392 peak areas were calculated and used to perform principle component analysis (PCA;
393 **Supplementary Table S3**). As expected, the analyses for the 0 and 72 h time points are well
394 separated on the PCA plot, whereas the analytical replicates are tightly clustered. The 0 h
395 data is also well clustered, but there is clear separation at 72h for each laboratory. The first
396 two principle components on the PCA scores plot (**Supplementary Fig. S6**) explain 85 % of
397 the variation. The first principle component demonstrates separation based on the time of
398 PAPC air exposure, whereas second principle component (explaining 18 % of the variation)

399 corresponds to separation based on inter-laboratory instrument variations; samples analysed
400 by L1 are grouped together at the bottom of the PCA scores plot, while L3 and L4 analysed
401 samples cluster more closely together. The minor variations explained by second principle
402 component (18%) are probably due to the type of mass analyzers used in the study (L1 - Q-
403 TOF mass spectrometer; L3 and L4 - quadrupole-Orbitrap MS).

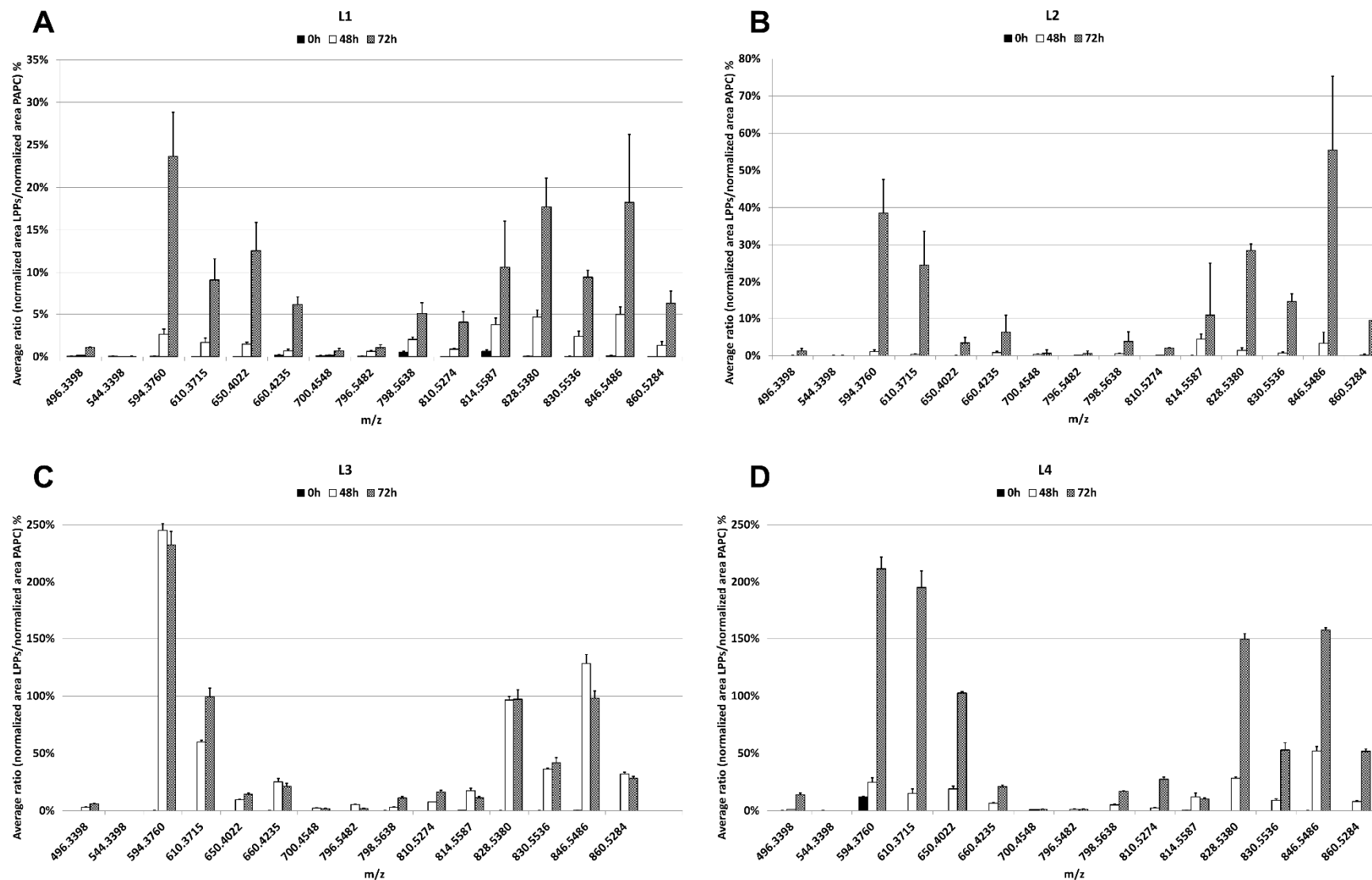
404 Furthermore, to compare the impact of sample preparation at different locations with
405 the variation in analysis of a single, centrally prepared sample analyzed in different
406 laboratories, we performed PCA of the normalized peak areas of the 72h samples generated
407 in L3 and analysed in L1 (labeled L1a) and L4 (labeled L4a) and the samples generated
408 independently by the four laboratories and analysed in those laboratories (L1, L2, L3, and
409 L4) (**Supplementary Tables S3 and S5, Fig. 4**). It is clear that the data for the sample
410 centrally generated in L3 but analysed at different locations cluster closely together and show
411 minimal variation, while the samples generated in different locations showed much higher
412 distribution. This demonstrates that the main variance was in the sample preparation, and that
413 the analysis of the same sample at different laboratories, using three different instruments
414 (L1:5600 TripleTOF, L3: Orbitrap Fusion™ Lumos™ Tribrid™ and L4: Q Exactive™
415 Plus), gave statistically very similar results. The reproducibility of analysis across the four
416 laboratories is supported by the 0 h data in **Supplementary Fig. S6**, which is also tightly
417 clustered.



418

419 **Fig. 4:** PCA scores plot for normalized LPPs peak area in sample generated at 72h in L3 and
 420 analysed in three different laboratories (L1a, L3 and L4a), and samples prepared
 421 independently in the four laboratories (L1, L2, L3, L4). Violet squares – L1, blue squares –
 422 L1a, blue stars – L2, pink circles – L3, yellow triangle – L4, orange triangle – L4a.

423 Combining the results of the relative quantification of 15 LPPs from oxPAPC
 424 preparations produced and analyzed independently in four different laboratories (**Fig. 5,**
 425 **Table 3** and **Supplementary Table S4**), six LPPs were among the most abundant signals in
 426 all labs and could be routinely identified and quantified, and therefore were chosen to serve
 427 as representatives of the oxPAPC mixture at the 48 and 72 h time points.



428

429

430

431

Fig. 5. Relative quantities (expressed as % of unmodified PAPC after the normalization to internal standard) of 15 representative LPPs from PAPC exposed to air oxidation for 0, 48 and 72 h. Graphs are shown for the time course at individual laboratories: L1 (A), L2 (B), L3 (C), and L4 (D) at 0 h, 48 h and 72 h. Identifications for each of the LPP masses can be found in **Supplementary Table S1**.

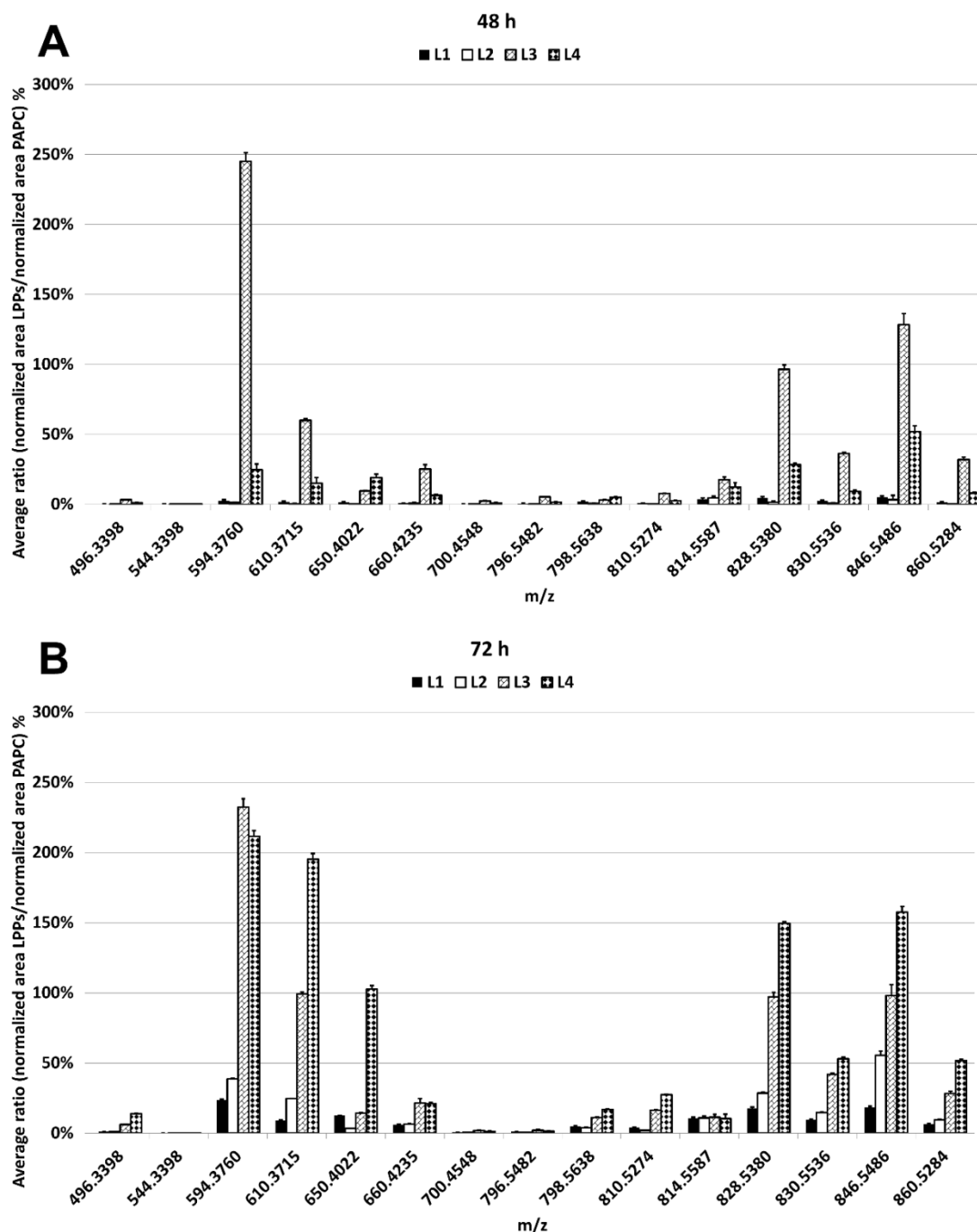
432 **Table 3.** The most abundant LPPs in air oxidized PAPC preparations for each laboratory (L1-
 433 L4) quantified relative to unmodified PAPC after normalization of corresponding peak areas
 434 to internal standard.

LPP, give as m/z values of protonated ions	L1	L2	L3	L4
594.38 ⁺	24 %		232 %	211 %
610.37 ⁺		39 %	99 %	195 %
650.40 ⁺	13 %	25 %		103 %
814.56 ⁺	11 %			
828.54 ⁺	18 %	28 %	97 %	149 %
830.55 ⁺		15 %	42 %	
846.55 ⁺	18 %	55 %	98 %	157 %

435
 436 These correspond to three short (m/z 594.38⁺, 610.37⁺, 650.40⁺), and three long chain
 437 (m/z 828.55⁺, 830.55⁺, 846.55⁺) LPPs. Based on the results of the MS/MS identifications, the
 438 short chain LPPs can be assigned to POVPC, PGPC and HOOAPC. For the long chain LPPs
 439 each m/z value, and thus elemental composition, can correspond to several isomeric species
 440 (**Table 2** and **Supplementary Table S1**). For instance, the LPP with elemental composition
 441 C₄₄H₇₈NO₁₁P (m/z 828.55⁺), usually referred to in oxPAPC mixtures as epoxyisoprostane E2
 442 containing PC (PEIPC), could also be represented by the following combinations of the
 443 functional groups on a long chain LPP derived from AA: [OOH and keto], [2OH and keto],
 444 [2 epoxy and keto], and [epoxy, OH and keto]. The LPPs with elemental compositions
 445 C₄₄H₈₀NO₁₁P (e.g. 3OH or OH + OOH) and C₄₄H₈₀NO₁₂P (e.g. 4OH or 2OOH) are clearly
 446 represented by a mixture of isomeric structures, as some of these were at least partially
 447 separated by chromatography in this study. However, for the relative quantification reported
 448 here the total peak area for each m/z were combined to report overall abundance of all of the
 449 LPP isomers in order to be comparable with previously reported values for oxPAPC
 450 mixtures, which have commonly been analyzed by direct infusion methods where the
 451 isomeric species have not been differentiated.

452 Although the most abundant LPPs were essentially the same between all four
 453 participating laboratories, the abundances of oxidized lipids relative to unmodified PAPC
 454 were quite different (**Fig. 6**). Thus, after 48 h air exposure the oxPAPC prepared in L3
 455 showed the highest oxidation levels, with POVPC being the most abundant LPP formed (245

456 % relative to unmodified PAPC). Among the long chain LPPs, the signals at m/z 846.55⁺
 457 (128 %) and 830.54⁺ (96 %) were the highest after 48 h of air exposure. After 72 h exposure
 458 to the air oxidation, the highest LPPs quantities were detected in L4, with POVPC (211 %),
 459 PGPC (195 %) and long chain LPPs at m/z 846.55⁺ (149 %) and 830.54⁺ (157 %) being the
 460 most abundant.



461
 462 **Fig. 6.** Relative quantities (expressed as % of unmodified PAPC after the normalization to
 463 internal standard) of 15 LPPs in PAPC exposed to the air oxidation comparing directly the
 464 relative quantities identified in L1, L2, L3, and L4 at 48 (A) and 72 h (B).

465 Thus, overall relative abundances for the same LPPs produced in four laboratories
 466 differed markedly across the time course, and by up to 13.5-fold (e.g. signal at m/z 828.55⁺ in
 467 L1 and L4) even after 72 h of PAPC oxidation. The most variation between laboratories was
 468 seen at the 48 h time point and by 72 h the profiles in L2, 3 and 4 showed relatively similar
 469 overall abundance of oxidized products, although still with significant variation in individual
 470 species. In L1 the overall level of oxidation was still low even after 72 h. ANOVA analysis
 471 (**Table S5**) confirmed the statistical significance of the differences, with p-values below 0.05
 472 for all quantified LPPs except PGPC at the 72 h time point.

473 One likely source of the difference in the oxidation rates could be small differences in
 474 the laboratory temperatures during PAPC air exposure, as average room temperatures in L1
 475 were 22-25 °C, L2 16 °C, L3 28 °C, and L4 25 °C; this could result in changes in the rate of
 476 the initiation of the free radical oxidation, which is then amplified by the radical chain
 477 reaction. The laboratory temperature at which air oxidation of oxPAPC is performed is
 478 usually not reported in publications and might be a significant confounder in reported results.
 479 However, this is clearly not the only reason, as the L1 had the lowest level of oxidation
 480 throughout, but was not the coldest laboratory. Most importantly from the point of view of
 481 experiments that are dependent on bioactivity, there is clearly significant variability in the
 482 rate of reaction and the distribution of oxidized products produced.

483

484 **Table 4.** “Truncation score” (TS) for the oxPAPC preparations from the four participating
 485 labs, calculated as the ratio between the summed abundances of three of the most abundant
 486 short chain LPPs (signal at m/z 594.38⁺, 610.37⁺, 650.40⁺) to three of the most abundant long
 487 chain LPPs (signals at m/z 828.54⁺, 830.55⁺, 846.55⁺).

	oxPAPC TS	
	48 h	72 h
L1	0.48	1.00
L2	0.28	0.68
L3	1.21	1.46
L4	0.66	1.41

488

489 In the literature, as a very general classification of bioactive compounds in air oxidized
 490 PAPC preparations, short chain LPPs are usually associated with pro-inflammatory effects
 491 whereas long chain LPPs are often associated with anti-inflammatory or protective functions

492 [17,24,25]. As is clear from the data presented above, despite the oxPAPC samples being
493 generated in the four different laboratories using the same protocol, which required minimal
494 sample manipulation (air exposure of the PAPC dried film), and each preparation giving rise
495 to approximately the same set of abundant LPPs, there was a high variability in the total
496 oxidation levels and in the extent of generation of individual LPPs. For this reason, a MS
497 based evaluation for all in-house produced oxPAPC mixtures would be beneficial to clarify
498 their exact composition before testing the biological effects.

499 Furthermore, a useful marker to help to characterize oxPAPC samples could be the ratio
500 of short to long chain oxidation products, which we suggest could be called the “truncation
501 score” (TS). This can be calculated for each oxPAPC preparation using the simple formula
502 $TS = \sum \% \text{ of short chain LPPs} / \sum \% \text{ of long chain LPPs}$. The TS calculated using, for
503 example, the three most abundant species from each classification (**Table 3**), would be
504 indicative of the ratio between short and long chain LPPs for each preparation, which is likely
505 to be one of the most important characteristics for bioactivity. A TS value equal to one would
506 indicate equal contribution of short and long chain LPPs, whereas $TS > 1$ and $TS < 1$ would
507 correspond to the prevalence of short or long chain LPPs, respectively. The results from this
508 study using the six most abundant species are shown in **Table 4**. This indicates that while the
509 overall oxidation levels from L2 and L4 at 72 h look similar in the base peak chromatograms
510 in **Fig. 1**, the preparation from L2 is higher in long chain components, while that for L4 is
511 higher in short chain. Therefore, although TS is a very rough estimation for the prevalence of
512 short over long chain LPPs, it could be used to evaluate the oxidation state balance of
513 oxPAPC preparations before using them in biological experiments. It is not necessary to
514 perform full LC-MS/MS characterization to determine the TS, as direct infusion MS data,
515 which are usually obtained to validate PAPC oxidation by air exposure for in-house
516 preparations, could be used.

517 One should also bear in mind that not it is not only the relative abundance of short
518 chain over the long chain LPPs important, but their absolute concentrations are also highly
519 significant. However, given the wide variety of chemical structures within oxPAPC mixture,
520 and thus differences in ionization efficiency of LPPs with various functional groups, pure
521 synthetic standards for each LPP class would be required to perform absolute quantification.

522 **4. Conclusions**

523 We have performed a multi-laboratory evaluation of air oxidized PAPC preparations
524 from four different laboratories using LC-MS/MS analysis, focusing on the identification and

525 relative quantification of the LPPs formed. High intra-sample reproducibility and a very
526 similar overall pattern of oxidation between the four laboratories was demonstrated.
527 However, significant differences in the general extent of lipid oxidation relative to
528 unmodified PAPC were observed. Thus, we propose that an MS based evaluation for all in
529 house produced oxPAPC mixtures should be performed before using them to study biological
530 effects of oxidized lipids. Furthermore, we suggest calculating the “truncation score” as a
531 rough estimation of the balance between short vs long chain products of arachidonic acid
532 oxidation.

533

534 **Acknowledgments**

535 Financial support from the EU H2020 funded project MASSTRPLAN (Grant number
536 675132; to all authors except TM) and German Federal Ministry of Education and Research
537 (BMBF) within the framework of the e:Med research and funding concept for SysMedOS
538 project (to MF) are gratefully acknowledged. Thanks are due to University of Aveiro, Marine
539 Lipidomics Laboratory, Fundação para a Ciência e a Tecnologia (FCT, MECPortugal),
540 European Union, QREN, Programa Operacional Factores de Competitividade (COMPETE)
541 and FEDER for the financial support to QOPNA (FCT UID/QUI/00062/2019) and CESAM
542 (UID/AMB/50017/2019) research units; Portuguese Mass Spectrometry Network (LISBOA-
543 01-0145-FEDER-402-022125), FCT/MEC through national funds, and the co-funding by the
544 FEDER, within the PT2020 Partnership Agreement and Compete 2020. We thank Prof. Ralf
545 Hoffmann (Institute of Bioanalytical Chemistry, University of Leipzig) for providing access
546 to his laboratory and Dr. Martin Zeller for scientific support and discussion.

547

548 **Conflict of interests**

549 The authors declare no conflict of interests.

550

551 **Bibliography**

552

- 553 [1] A. Trpkovic, I. Resanovic, J. Stanimirovic, D. Radak, S.A. Mousa, D. Cenic-
554 Milosevic, D. Jevremovic, E.R. Isenovic, Oxidized low-density lipoprotein as a
555 biomarker of cardiovascular diseases., *Crit. Rev. Clin. Lab. Sci.* 52 (2015) 70–85.
556 doi:10.3109/10408363.2014.992063.
- 557 [2] D. Hasanally, A. Edel, R. Chaudhary, A. Ravandi, Identification of Oxidized

- 558 Phosphatidylinositols Present in OxLDL and Human Atherosclerotic Plaque., *Lipids*.
559 52 (2017) 11–26. doi:10.1007/s11745-016-4217-y.
- 560 [3] H. Itabe, K. Suzuki, Y. Tsukamoto, R. Komatsu, M. Ueda, M. Mori, Y. Higashi, T.
561 Takano, Lysosomal accumulation of oxidized phosphatidylcholine-apolipoprotein B
562 complex in macrophages: intracellular fate of oxidized low density lipoprotein.,
563 *Biochim. Biophys. Acta*. 1487 (2000) 233–245.
- 564 [4] V.N. Bochkov, Inflammatory profile of oxidized phospholipids., *Thromb. Haemost.* 97
565 (2007) 348–354.
- 566 [5] M. Aldrovandi, V.B. O’Donnell, Oxidized PLs and vascular inflammation., *Curr.*
567 *Atheroscler. Rep.* 15 (2013) 323. doi:10.1007/s11883-013-0323-y.
- 568 [6] N. Leitinger, Oxidized phospholipids as triggers of inflammation in atherosclerosis.,
569 *Mol. Nutr. Food Res.* 49 (2005) 1063–1071. doi:10.1002/mnfr.200500086.
- 570 [7] N. Leitinger, The role of phospholipid oxidation products in inflammatory and
571 autoimmune diseases: evidence from animal models and in humans., *Subcell.*
572 *Biochem.* 49 (2008) 325–350. doi:10.1007/978-1-4020-8830-8_12.
- 573 [8] V.B. O’Donnell, M. Aldrovandi, R.C. Murphy, G. Kronke, Enzymatically oxidized
574 phospholipids assume center stage as essential regulators of innate immunity and cell
575 death., *Sci. Signal.* 12 (2019). doi:10.1126/scisignal.aau2293.
- 576 [9] J.A. Berliner, N. Leitinger, S. Tsimikas, The role of oxidized phospholipids in
577 atherosclerosis., *J. Lipid Res.* 50 (2009) S207-12. doi:10.1194/jlr.R800074-JLR200.
- 578 [10] B. Burla, M. Arita, M. Arita, A.K. Bendt, A. Cazenave-Gassiot, E.A. Dennis, K.
579 Ekroos, X. Han, K. Ikeda, G. Liebisch, M.K. Lin, T.P. Loh, P.J. Meikle, M. Orešič, O.
580 Quehenberger, A. Shevchenko, F. Torta, M.J.O. Wakelam, C.E. Wheelock, M.R.
581 Wenk, MS-based lipidomics of human blood plasma: a community-initiated position
582 paper to develop accepted guidelines, *J. Lipid Res.* 59 (2018) 2001–2017.
583 doi:10.1194/jlr.S087163.
- 584 [11] E.A. Dennis, P.C. Norris, Eicosanoid storm in infection and inflammation, *Nat. Rev.*
585 *Immunol.* (2015) 511–523. doi:10.1038/nri3859.
- 586 [12] S. Yedgar, M. Krimsky, Y. Cohen, R.J. Flower, Treatment of inflammatory diseases
587 by selective eicosanoid inhibition: a double-edged sword?, *Trends Pharmacol. Sci.* 28

- 588 (2007) 459–464. doi:10.1016/j.tips.2007.07.005.
- 589 [13] P. Bretscher, J. Egger, A. Shamshiev, M. Trotsmuller, H. Kofeler, E.M. Carreira, M.
590 Kopf, S. Freigang, Phospholipid oxidation generates potent anti-inflammatory lipid
591 mediators that mimic structurally related pro-resolving eicosanoids by activating Nrf2,
592 EMBO Mol. Med. 7 (2015) 593–607. doi:10.15252/emmm.201404702.
- 593 [14] A.D. Watson, N. Leitinger, M. Navab, K.F. Faull, S. Hörkkö, J.L. Witztum, W.
594 Palinski, D. Schwenke, R.G. Salomon, W. Sha, G. Subbanagounder, A.M. Fogelman,
595 J.A. Berliner, Structural identification by mass spectrometry of oxidized phospholipids
596 in minimally oxidized low density lipoprotein that induce monocyte/endothelial
597 interactions and evidence for their presence in vivo, J. Biol. Chem. 272 (1997) 13597–
598 13607. doi:10.1074/jbc.272.21.13597.
- 599 [15] N. Leitinger, T.R. Tyner, L. Oslund, C. Rizza, G. Subbanagounder, H. Lee, P.T. Shih,
600 N. Mackman, G. Tigyi, M.C. Territo, J.A. Berliner, D.K. Vora, Structurally similar
601 oxidized phospholipids differentially regulate endothelial binding of monocytes and
602 neutrophils, Proc. Natl. Acad. Sci. 96 (1999) 12010–12015.
603 doi:10.1073/pnas.96.21.12010.
- 604 [16] Y. Ke, N. Zebda, O. Oskolkova, T. Afonyushkin, E. Berdyshev, Y. Tian, F. Meng, N.
605 Sarich, V.N. Bochkov, J.M. Wang, A.A. Birukova, K.G. Birukov, Anti-Inflammatory
606 Effects of OxPAPC Involve Endothelial Cell-Mediated Generation of LXA4, Circ.
607 Res. 121 (2017) 244–257. doi:10.1161/CIRCRESAHA.116.310308.
- 608 [17] A.A. Birukova, V. Starosta, X. Tian, K. Higginbotham, L. Koroniak, J.A. Berliner,
609 K.G. Birukov, Fragmented oxidation products define barrier disruptive endothelial cell
610 response to OxPAPC, Transl. Res. 161 (2013) 495–504.
611 doi:10.1016/j.trsl.2012.12.008.
- 612 [18] N. Sarich, X. Tian, G. Gawlak, A.A. Birukova, K.G. Birukov, D.B. Sacks, Y. Tian,
613 Role of IQGAP1 in endothelial barrier enhancement caused by OxPAPC, Am. J.
614 Physiol. Cell. Mol. Physiol. 311 (2016) L800–L809. doi:10.1152/ajplung.00095.2016.
- 615 [19] C. Martin, C. Stoffer, M. Mohammadi, J. Hugo, E. Leipold, B. Oehler, H.L. Rittner, R.
616 Blum, NaV1.9 Potentiates Oxidized Phospholipid-Induced TRP Responses Only under
617 Inflammatory Conditions, Front. Mol. Neurosci. 11:7 (2018).
618 doi:10.3389/fnmol.2018.00007.

- 619 [20] B. Oehler, K. Kistner, C. Martin, J. Schiller, R. Mayer, M. Mohammadi, R.S. Sauer,
620 M.R. Filipovic, F.R. Nieto, J. Kloka, D. Pflücke, K. Hill, M. Schaefer, M. Malcangio,
621 P.W. Reeh, A. Brack, R. Blum, H.L. Rittner, Inflammatory pain control by blocking
622 oxidized phospholipid-mediated TRP channel activation, *Sci. Rep.* 7: 5447 (2017).
623 doi:10.1038/s41598-017-05348-3.
- 624 [21] I. Zanoni, Y. Tan, M. Di Gioia, J.R. Springstead, J.C. Kagan, By Capturing
625 Inflammatory Lipids Released from Dying Cells, the Receptor CD14 Induces
626 Inflammasome-Dependent Phagocyte Hyperactivation, *Immunity.* 47 (2017) 697–709.
627 doi:10.1016/j.immuni.2017.09.010.
- 628 [22] I. Zanoni, Y. Tan, M. Di Gioia, A. Broggi, J. Ruan, J. Shi, C.A. Donado, F. Shao, H.
629 Wu, J.R. Springstead, J.C. Kagan, An endogenous caspase-11 ligand elicits
630 interleukin-1 release from living dendritic cells, *Science* (80-.). 352 (2016) 1232–
631 1236. doi:10.1126/science.aaf3036.
- 632 [23] L.H. Chu, M. Indramohan, R.A. Ratsimandresy, A. Gangopadhyay, E.P. Morris, D.M.
633 Monack, A. Dorfleutner, C. Stehlik, The oxidized phospholipid oxPAPC protects from
634 septic shock by targeting the non-canonical inflammasome in macrophages, *Nat.*
635 *Commun.* 9:996 (2018). doi:10.1038/s41467-018-03409-3.
- 636 [24] P. Karki, K.G. Birukov, Lipid mediators in the regulation of endothelial barriers.,
637 *Tissue Barriers.* 6 (2018) e1385573. doi:10.1080/21688370.2017.1385573.
- 638 [25] V. Bochkov, B. Gesslbauer, C. Mauerhofer, M. Philippova, P. Erne, O. V. Oskolkova,
639 Pleiotropic effects of oxidized phospholipids, *Free Radic. Biol. Med.* 111 (2017) 6–24.
640 doi:10.1016/j.freeradbiomed.2016.12.034.
- 641 [26] C. Mauerhofer, M. Philippova, O. V Oskolkova, V.N. Bochkov, Hormetic and anti-
642 inflammatory properties of oxidized phospholipids., *Mol. Aspects Med.* 49 (2016) 78–
643 90. doi:10.1016/j.mam.2016.02.003.
- 644 [27] A. Criscuolo, M. Zeller, K. Cook, G. Angelidou, M. Fedorova, Rational selection of
645 reverse phase columns for high throughput LC-MS lipidomics., *Chem. Phys. Lipids.*
646 221 (2019) 120–127. doi:10.1016/j.chemphyslip.2019.03.006.
- 647 [28] Z. Ni, G. Angelidou, R. Hoffmann, M. Fedorova, LPPtiger software for lipidome-
648 specific prediction and identification of oxidized phospholipids from LC-MS datasets,

- 649 Sci. Rep. 7: 15138 (2017). doi:10.1038/s41598-017-15363-z.
- 650 [29] B. Davis, G. Koster, L.J. Douet, M. Scigelova, G. Woffendin, J.M. Ward, A. Smith, J.
651 Humphries, K.G. Burnand, C.H. Macphee, A.D. Postle, Electrospray ionization mass
652 spectrometry identifies substrates and products of lipoprotein-associated phospholipase
653 A2 in oxidized human low density lipoprotein, *J. Biol. Chem.* 283 (2008) 6428–6437.
654 doi:10.1074/jbc.M709970200.
- 655 [30] E.A. Podrez, E. Poliakov, Z. Shen, R. Zhang, Y. Deng, M. Sun, P.J. Finton, L. Shan,
656 M. Febbraio, D.P. Hajjar, R.L. Silverstein, H.F. Hoff, R.G. Salomon, S.L. Hazen, A
657 novel family of atherogenic oxidized phospholipids promotes macrophage foam cell
658 formation via the scavenger receptor CD36 and is enriched in atherosclerotic lesions, *J.*
659 *Biol. Chem.* 277 (2002) 38517–38523. doi:10.1074/jbc.M205924200.
- 660 [31] E. Fahy, S. Subramaniam, R.C. Murphy, M. Nishijima, C.R.H. Raetz, T. Shimizu, F.
661 Spener, G. van Meer, M.J.O. Wakelam, E.A. Dennis, Update of the LIPID MAPS
662 comprehensive classification system for lipids, *J. Lipid Res.* 50 (2009) S9–S14.
663 doi:10.1194/jlr.R800095-JLR200.
- 664 [32] M. Lange, Z. Ni, A. Criscuolo, M. Fedorova, *Liquid Chromatography Techniques in*
665 *Lipidomics Research, Chromatographia.* 82 (2019) 77–100. doi:10.1007/s10337-018-
666 3656-4.
- 667 [33] H. Nakanishi, Y. Iida, T. Shimizu, R. Taguchi, Separation and quantification of sn-1
668 and sn-2 fatty acid positional isomers in phosphatidylcholine by RPLC-ESIMS/MS, *J.*
669 *Biochem.* 147 (2010) 245–256. doi:10.1093/jb/mvp171.
- 670 [34] K. Wozny, W.D. Lehmann, M. Wozny, B.S. Akbulut, B. Brügger, A method for the
671 quantitative determination of glycerophospholipid regioisomers by UPLC-ESI-
672 MS/MS, *Anal. Bioanal. Chem.* 411 (2019) 915–924. doi:10.1007/s00216-018-1517-5.
- 673 [35] A.C. Almstrand, C. Johnson, R.C. Murphy, Evidence for an N-methyl transfer reaction
674 in phosphatidylcholines with a terminal aldehyde during negative electrospray
675 ionization tandem mass spectrometry, *Anal. Bioanal. Chem.* 407 (2015) 5045–52.
676 doi:10.1007/s00216-015-8555-z.
- 677 [36] G. Subbanagounder, J.W. Wong, H. Lee, K.F. Faull, E. Miller, J.L. Witztum, J.A.
678 Berliner, Epoxyisoprostane and epoxycyclopentenone phospholipids regulate

- 679 monocyte chemotactic protein-1 and interleukin-8 synthesis. Formation of these
680 oxidized phospholipids in response to interleukin-1 β , *J. Biol. Chem.* 277 (2002) 7271–
681 81. doi:10.1074/jbc.M107602200.
- 682 [37] E. Rampler, A. Criscuolo, M. Zeller, Y. El Abiead, H. Schoeny, G. Hermann, E.
683 Sokol, K. Cook, D.A. Peake, B. Delanghe, G. Koellensperger, A novel lipidomics
684 workflow for improved human plasma identification and quantification using RPLC-
685 MSn methods and isotope dilution strategies, *Anal. Chem.* 90 (2017) 6494–6501.
686 doi:10.1021/acs.analchem.7b05382.
- 687 [38] V.N. Bochkov, O. V. Oskolkova, K.G. Birukov, A.-L. Levonen, C.J. Binder, J. Stöckl,
688 Generation and Biological Activities of Oxidized Phospholipids, *Antioxid. Redox*
689 *Signal.* 12 (2009) 1009–1059. doi:10.1089/ars.2009.2597.

690

Highlights

- Multi-laboratory evaluation of air oxidized PAPC preparations by LC-MS/MS.
- Identification and relative quantification of lipid peroxidation products (LPPs).
- oxPAPC preparations should be characterized by MS prior testing biological effects of oxidized lipids.
- “Truncation score” is proposed as a rough estimation of oxPAPC oxidation status.